

Top-quark couplings at current and future colliders

ECFA tt-threshold meeting

17th April 2024

Víctor Miralles

in collaboration (currently) with:

F. Cornet-Gómez, Marcos Miralles López,
María Moreno Llácer, Marcel Vos



The University of Manchester

Introduction

- Our goal is to constrain all the top-quark related Wilson coefficients of the SMEFT
- The fits have been performed using HEPfit [\[1910.14012\]](#)
- Estimations on the improvement of the measurements are presented for the HL-LHC
- Estimation for the relevant observables for this fit in future e^+e^- colliders are shown
- Prospects for our limits in the HL-LHC and a future e^+e^- colliders are obtained

SMEFT operators relevant for the top-quark

2-quark operators

Couplings of the t- and b-quark to the Z

$$O_{\varphi Q}^3 \equiv (\bar{Q} \tau^I \gamma^\mu Q) (\varphi^\dagger i \overleftrightarrow{D}_\mu^I \varphi)$$

$$O_{\varphi Q}^1 \equiv (\bar{Q} \gamma^\mu Q) (\varphi^\dagger i \overleftrightarrow{D}_\mu \varphi)$$

$$O_{\varphi t(b)} \equiv (\bar{t}(b) \gamma^\mu t(b)) (\varphi^\dagger i \overrightarrow{D}_\mu \varphi)$$

EW dipole operators

$$O_{uW} \equiv (\bar{Q} \tau^I \sigma^{\mu\nu} t) (\varepsilon \varphi^* W_{\mu\nu}^I)$$

$$O_{tB} \equiv (\bar{Q} \sigma^{\mu\nu} t) (\varepsilon \varphi^* B_{\mu\nu})$$

Chromo-magnetic dipole op.

t-quark yukawa

$$O_{tG} \equiv (\bar{Q} \sigma^{\mu\nu} T^A t) (\varepsilon \varphi^* G_{\mu\nu}^A)$$

$$O_{t\varphi} \equiv (\bar{Q} t) (\varepsilon \varphi^* \varphi^\dagger \varphi)$$

4-quark operators

Couplings of light quarks with t- and b-quarks

$$O_{tu}^8$$

$$O_{td}^8$$

$$O_{Qq}^{1,8}$$

$$O_{Qu}^8$$

$$O_{Qd}^8$$

$$O_{Qq}^{3,8}$$

$$O_{tq}^8$$

2-quark 2-lepton operators

Couplings of light leptons with t- and b-quarks

$$O_{eb}$$

$$O_{lb}$$

$$O_{et}$$

$$O_{lt}$$

$$O_{eQ}$$

$$O_{IQ}^+$$

$$O_{IQ}^-$$

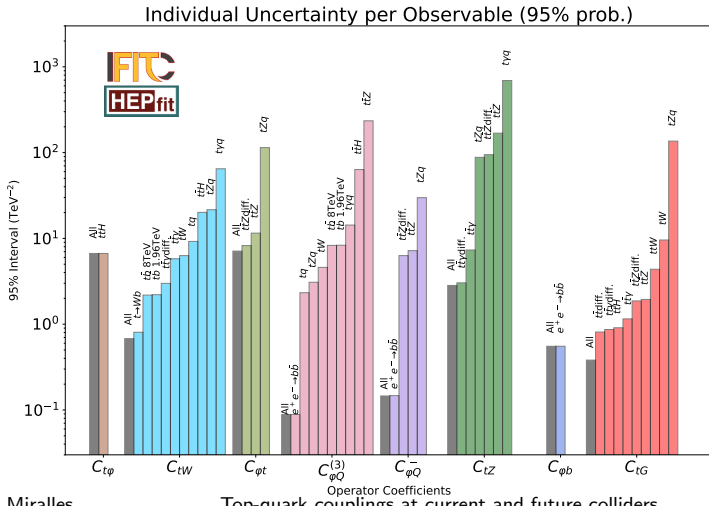
Observables from current colliders (LEP/SLC, Tevatron, LHC run 1 & 2)

- Here we show the observables included that have been measured in the actual colliders
- The parametrisations have been obtained using SMEFT@NLO in madgraph

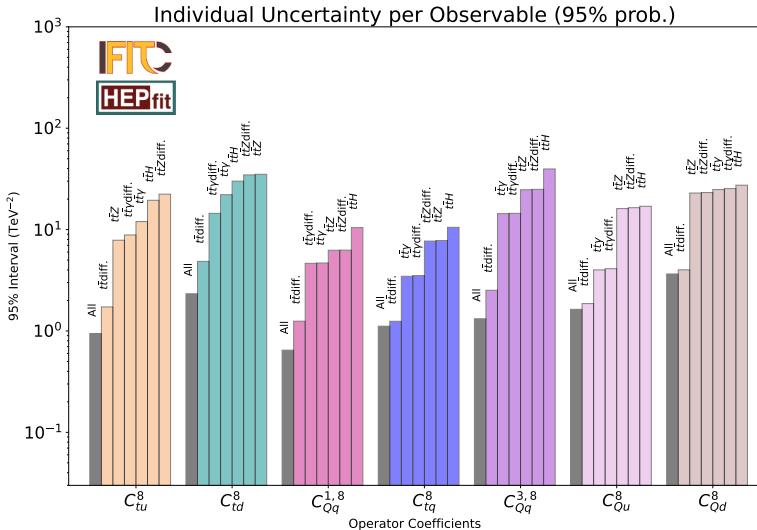
| Process | Observable | \sqrt{s} | $\int \mathcal{L}$ | Experiment |
|--|-------------------------------------|---------------|------------------------|------------|
| $pp \rightarrow t\bar{t}$ | $d\sigma/dm_{t\bar{t}}$ (15+3 bins) | 13 TeV | 140 fb^{-1} | CMS |
| $pp \rightarrow t\bar{t}$ | $dA_C/dm_{t\bar{t}}$ (4+2 bins) | 13 TeV | 140 fb^{-1} | ATLAS |
| $pp \rightarrow t\bar{t}Z$ | $d\sigma/dp_T^Z$ (7 bins) | 13 TeV | 140 fb^{-1} | ATLAS |
| $pp \rightarrow t\bar{t}\gamma$ | $d\sigma/dp_T^\gamma$ (11 bins) | 13 TeV | 140 fb^{-1} | ATLAS |
| $pp \rightarrow t\bar{t}H + tHq$ | σ | 13 TeV | 140 fb^{-1} | ATLAS |
| $pp \rightarrow tZq$ | σ | 13 TeV | 77.4 fb^{-1} | CMS |
| $pp \rightarrow t\gamma q$ | σ | 13 TeV | 36 fb^{-1} | CMS |
| $pp \rightarrow t\bar{t}W$ | σ | 13 TeV | 36 fb^{-1} | CMS |
| $pp \rightarrow t\bar{b}$ (s-ch) | σ | 8 TeV | 20 fb^{-1} | LHC |
| $pp \rightarrow tW$ | σ | 8 TeV | 20 fb^{-1} | LHC |
| $pp \rightarrow tq$ (t-ch) | σ | 8 TeV | 20 fb^{-1} | LHC |
| $t \rightarrow Wb$ | F_0, F_L | 8 TeV | 20 fb^{-1} | LHC |
| $p\bar{p} \rightarrow t\bar{b}$ (s-ch) | σ | 1.96 TeV | 9.7 fb^{-1} | Tevatron |
| $e^- e^+ \rightarrow b\bar{b}$ | R_b, A_{FBLR}^{bb} | ~ 91 GeV | 202.1 pb^{-1} | LEP/SLD |

Current individual constraints on 2-quark operators

The basis is rotated following the prescription of the LHC top-quark working group: $C_{tZ} = \cos \theta_W C_{tW} - \sin \theta_W C_{tB}$, $C_{\phi Q}^- = C_{\phi Q}^{(1)} - C_{\phi Q}^{(3)}$

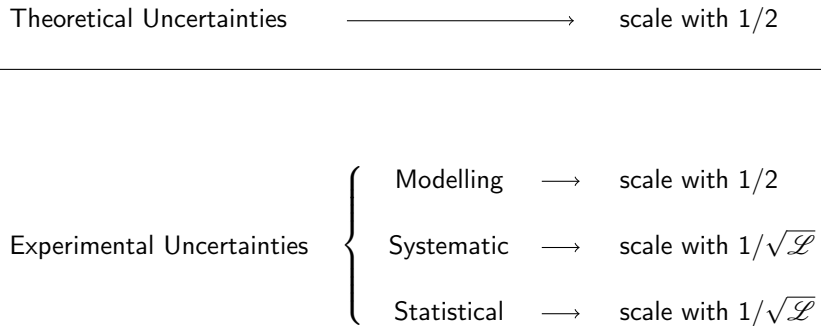


Current individual constraints on 4-quark operators



High Luminosity LHC

Prospects for Measurements at HL-LHC



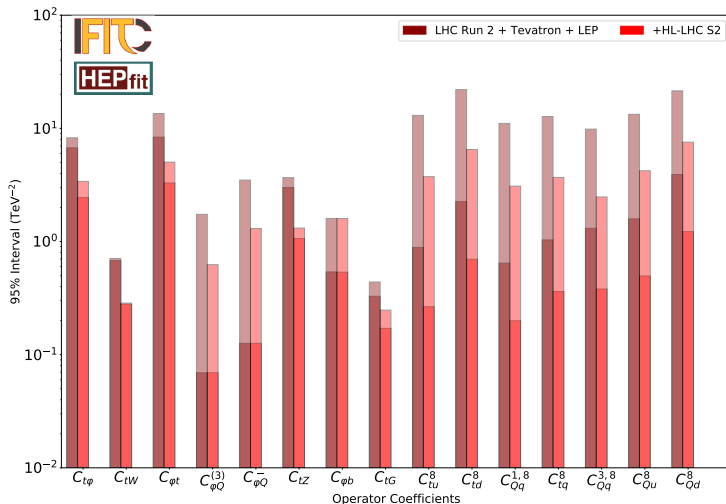
Prospects for Measurements at HL-LHC

Inclusive cross sections and helicities

| Process | Measured (fb) | SM (fb) | LHC Unc. | | | | | HL-LHC Unc. | | | | |
|--|---------------|---------|----------|-------|-------|-------|-------|-------------|--------|--------|-------|-------|
| | | | theo. | exp. | | | | theo. | exp. | | | |
| | | | | stat. | sys. | mod. | tot. | | stat. | sys. | mod. | tot. |
| $pp \rightarrow t\bar{t}H + t\bar{t}q$ | 640 | 664.3 | 41.7 | 90 | 40 | 70.7 | 121.2 | 20.9 | 19.4 | 8.6 | 35.4 | 41.3 |
| $pp \rightarrow t\bar{t}Z$ | 990 | 810.9 | 85.8 | 51.5 | 48.9 | 67.3 | 97.8 | 42.9 | 11.1 | 10.6 | 33.6 | 37.0 |
| $pp \rightarrow t\bar{t}\gamma$ | 39.6 | 38.5 | 1.76 | 0.8 | 1.25 | 2.16 | 2.62 | 0.88 | 0.17 | 0.27 | 1.08 | 1.13 |
| $pp \rightarrow tZq$ | 111 | 102 | 3.5 | 13.0 | 6.1 | 6.2 | 15.7 | 1.75 | 2.09 | 0.98 | 3.1 | 3.87 |
| $pp \rightarrow t\gamma q$ | 115.7 | 81 | 4 | 17.1 | 21.1 | 21.1 | 34.4 | 2 | 1.9 | 2.3 | 10.6 | 11.0 |
| $pp \rightarrow t\bar{t}W + \text{EW}$ | 770 | 647.5 | 76.1 | 120 | 59.6 | 73.0 | 152.6 | 38.1 | 13.1 | 6.5 | 36.5 | 39.4 |
| $pp \rightarrow t\bar{b}$ (s-ch) | 4900 | 5610 | 220 | 784 | 936 | 790 | 1454 | 110 | 35 | 42 | 395 | 399 |
| $pp \rightarrow tW$ | 23100 | 22370 | 1570 | 1086 | 2000 | 2773 | 3587 | 785 | 49 | 89 | 1386 | 1390 |
| $pp \rightarrow tq$ (t-ch) | 87700 | 84200 | 250 | 1140 | 3128 | 4766 | 5810 | 125 | 51 | 140 | 2383 | 2390 |
| F_0 | 0.693 | 0.687 | 0.005 | 0.009 | 0.006 | 0.009 | 0.014 | 0.003 | 0.0004 | 0.0003 | 0.004 | 0.004 |
| F_L | 0.315 | 0.311 | 0.005 | 0.006 | 0.003 | 0.008 | 0.011 | 0.003 | 0.0003 | 0.0002 | 0.004 | 0.004 |

Current constraints vs expected HL-LHC constraints

Shadowed (solid) bars → marginalised from global (individual) fit



Future lepton colliders

Measurements at lepton colliders: $b\bar{b}$ production

| Machine | Polarisation | Energy | Luminosity | Observable |
|-------------|--|-------------|----------------------------|---|
| ILC | $P(e^+, e^-):(-30\%, +80\%)$ $P(e^+, e^-):(+30\%, -80\%)$ | 250 GeV | 2 ab^{-1} | $\sigma_{b\bar{b}}$ A_{bb}^{bb} A_{FB}^{bb} |
| | | 500 GeV | 4 ab^{-1} | |
| | | 1 TeV | 8 ab^{-1} | |
| CLIC | $P(e^+, e^-):(0\%, +80\%)$ $P(e^+, e^-):(0\%, -80\%)$ | 380 GeV | 2 ab^{-1} | $\sigma_{b\bar{b}}$ A_{bb}^{bb} A_{FB}^{bb} |
| | | 1.5 TeV | 2.5 ab^{-1} | |
| | | 3 TeV | 5 ab^{-1} | |
| CEPC/FCC-ee | Unpolarised | Z-pole | $57.5/150 \text{ ab}^{-1}$ | $\sigma_{b\bar{b}}$ A_{bb}^{bb} A_{FB}^{bb} |
| | | 240 GeV | $20/5 \text{ ab}^{-1}$ | |
| | | 360/365 GeV | $1/1.5 \text{ ab}^{-1}$ | |

- Expected uncertainties from A. Irles, R. Pöschl, F. Richard
- These observables set constraints on the EW precision observables $C_{\varphi Q}^+ = C_{\varphi Q}^1 + C_{\varphi Q}^3$ and $C_{\varphi b}$
- Also relevant for 2-quark 2-lepton operators C_{IQ}^+ , C_{lb} and C_{eb}
- The higher-energy measurement are more relevant for the 2-quark 2-lepton operators

Measurements at lepton colliders: $t\bar{t}$ production

| Machine | Polarisation | Energy | Luminosity | Observable |
|-------------|------------------------------|---------|-------------------------|---------------------|
| ILC | $P(e^+, e^-):(-30\%, +80\%)$ | 500 GeV | 4 ab^{-1} | Optimal Observables |
| | $P(e^+, e^-):(+30\%, -80\%)$ | 1 TeV | 8 ab^{-1} | |
| CLIC | $P(e^+, e^-):(0\%, +80\%)$ | 380 GeV | 2 ab^{-1} | Optimal Observables |
| | $P(e^+, e^-):(0\%, -80\%)$ | 1.5 TeV | 2.5 ab^{-1} | |
| | | 3 TeV | 5 ab^{-1} | |
| CEPC/FCC-ee | Unpolarised | 350 GeV | 0.2 ab^{-1} | Optimal Observables |
| | | 365 GeV | $1/1.5 \text{ ab}^{-1}$ | |
| MuC | Unpolarised | 3 TeV | 1 ab^{-1} | Optimal Observables |
| | | 10 TeV | 10 ab^{-1} | |
| | | 30 TeV | 90 ab^{-1} | VBF |

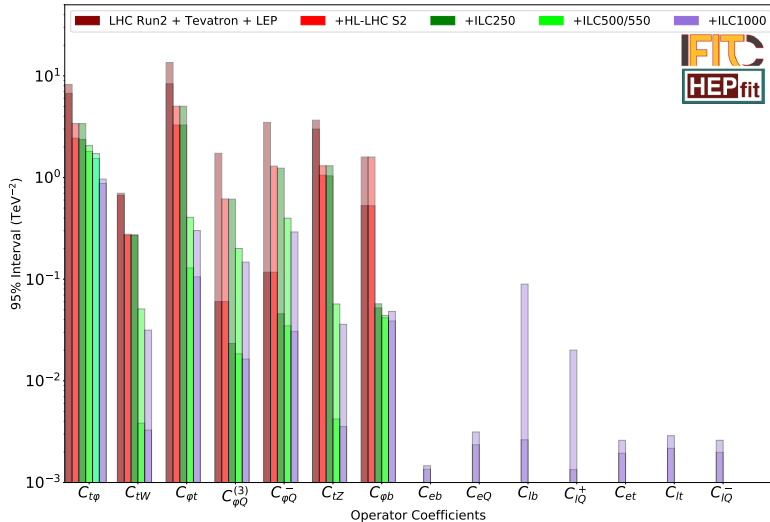
- Optimal observables maximally exploit the information in the fully differential $e^+e^- \rightarrow t\bar{t} \rightarrow bW^+\bar{b}W^-$ distribution [1807.02121]
- These constrain the 2-fermion operators $C_{\varphi Q}^-$, $C_{\varphi t}$, C_{tW} and C_{tZ}
- Also the 2-quark 2-lepton operators C_{IQ}^- , C_{lt} , C_{et} and C_{eQ}
- With these we eliminate blind directions in the $C_{\varphi Q}^{(1)} - C_{\varphi Q}^{(3)}$ plane

Measurements at lepton colliders: $t\bar{t}H$ production

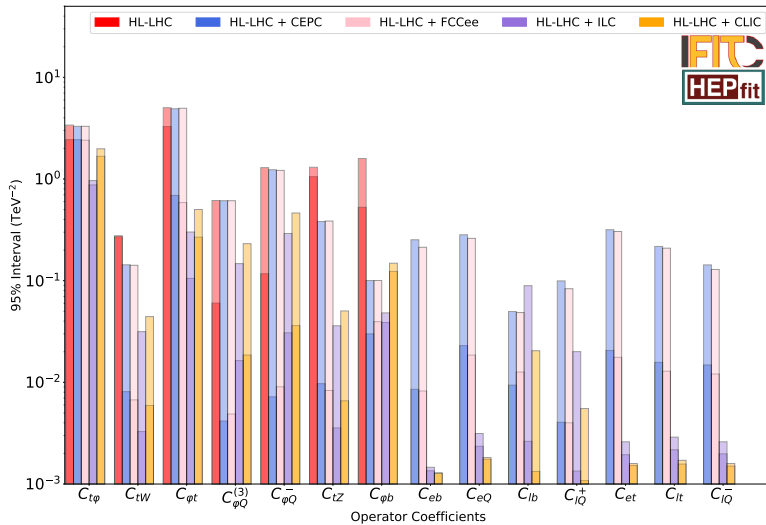
| Machine | Polarisation | Energy | Luminosity | Observable |
|---------|--|-------------|-----------------------|-------------------------|
| ILC | $P(e^+, e^-):(-30%, +80\%)$ | 500/550 GeV | 4 ab^{-1} | Inclusive cross section |
| | $P(e^+, e^-):(+30%, -80\%)$ | 1 TeV | 8 ab^{-1} | |
| CLIC | $P(e^+, e^-):(0\%, +80\%)$ $P(e^+, e^-):(0\%, -80\%)$ | 1.5 TeV | 2.5 ab^{-1} | Inclusive cross section |

- Essential measurement in order to improve the limits on the top-quark Yukawa
- The effect of a ILC run at 550 GeV has been studied
- At ILC550 the production cross section increases a factor of 3 w.r.t. ILC500 improving the statistical sensitivity by more than a 50%
- ILC550 and CLIC1500 have a similar sensitivity as HL-LHC
- ILC1000 improves the expected HL-LHC sensitivity by a factor of two

Expected constraints for different e^+e^- operation energies



Comparison of future colliders

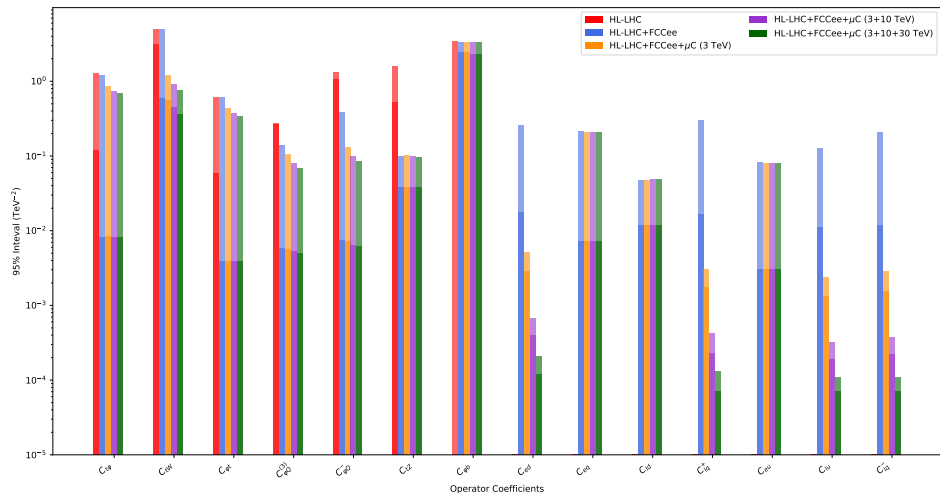


Top-quark Yukawa coupling uncertainties

| Values in % units | LHC | HL-LHC | ILC500 | ILC550 | ILC1000 | CLIC |
|-------------------|------------|--------|--------|--------|---------|------|
| δy_t | Global fit | 12.2 | 5.06 | 3.14 | 2.60 | 1.48 |
| | Indiv. fit | 10.20 | 3.70 | 2.82 | 2.34 | 1.41 |
| | | | | | | 2.56 |

- Since the sensitivity at ILC500 is worse than in HL-LHC there is no a huge improvement for the individual constraint
- For the global fit the improvement is relevant even for ILC500, thanks to constraining the Yukawa with more than one observable
- Increasing the energy by 50 GeV provides an important improvement in the constraints thanks to the growth in the cross section
- Similar results are found for CLIC
- An improvement higher than a factor of 2.5 would be obtain at the final stage of ILC w.r.t. the HL-LHC

Muon Collider limits



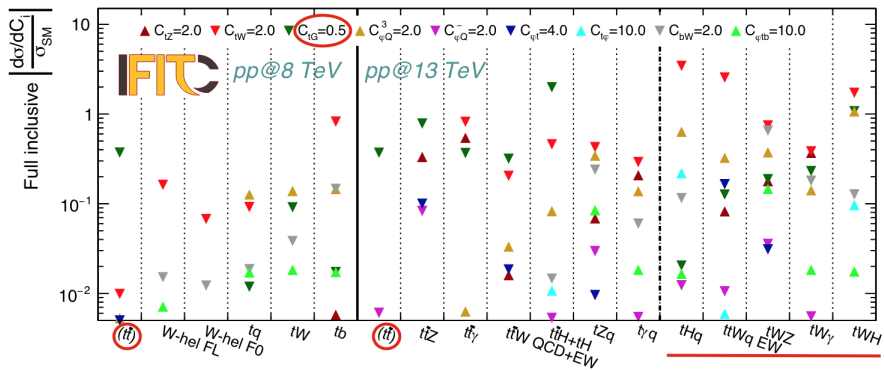
Summary

- HL-LHC expected to improve the bounds by roughly a factor 3 w.r.t. current state-of-the-art LHC run 2 + Tevatron + LEP/SLC
- An e^+e^- collider can significantly improve bounds on bottom-quark operators, and on top-quark operators if operated above the $t\bar{t}$ threshold
- Circular colliders (FCCee and CECP) operated at and slightly above the $t\bar{t}$ threshold can improve bottom- and top- operators by factor 5 and 2 for 2-fermion operators.
- Power to constrain 4-fermion operators limited by energy reach
- Linear colliders (ILC and CLIC) operated at two center-of-mass energies above the $t\bar{t}$ threshold can provide very tight bounds on all operators, with bounds on 4F taking advantage of energy-growing sensitivity
- Significant improvements for the limits on the top-quark yukawa are found when operating above 550 GeV

Thank you!

Back up

Sensitivity

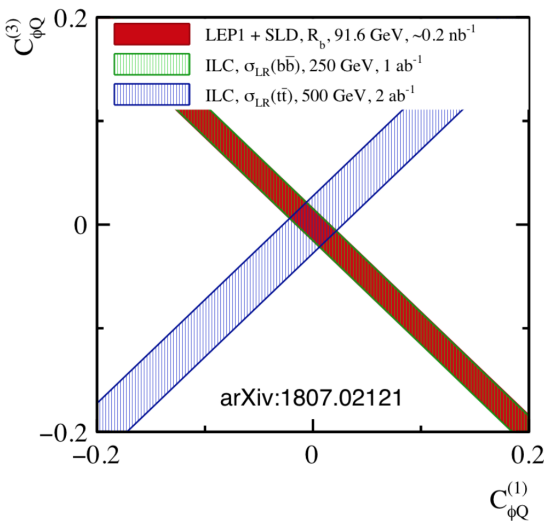


Future Colliders - Complementarity on e^+e^- Colliders

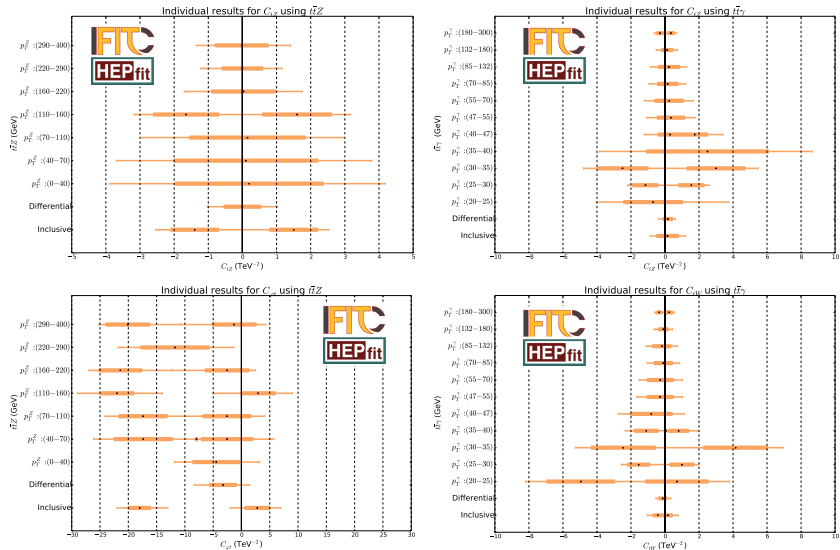
Good complementarity between $b\bar{b}$ (LEP) and $t\bar{t}$ (future e^+e^- collider) if we reach $\sqrt{s} > 2m_t$

$$\delta g_L^t = -(C_{\phi Q}^1 - C_{\phi Q}^3)m_t^2/\Lambda^2$$

$$\delta g_L^b = -(C_{\phi Q}^1 + C_{\phi Q}^3)m_t^2/\Lambda^2$$

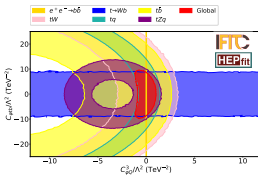
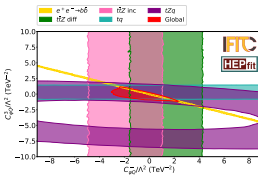
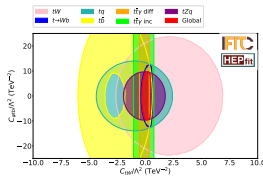
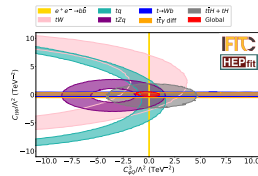
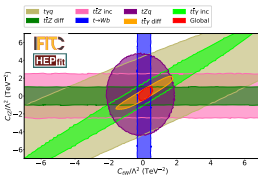
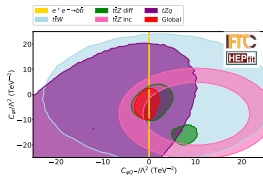


Results - Differential Cross Section Effect



Results - Complementarity Between Observables

- Very good complementarity between the observables
 - The data set is diverse enough to avoid the existence of blind directions



Dependencies

[1910.03606]

| parameter | $t\bar{t}$ | single t | tW | tZ | t decay | $t\bar{t}Z$ | $t\bar{t}W$ |
|----------------------|-------------------------------|-------------------------------|----------------|-------------------------------|-------------------------------|-------------------------------|-------------------------------|
| $C_{Qq}^{1,8}$ | Λ^{-2} | — | — | — | — | Λ^{-2} | Λ^{-2} |
| $C_{Qq}^{3,8}$ | Λ^{-2} | $\Lambda^{-4} [\Lambda^{-2}]$ | — | $\Lambda^{-4} [\Lambda^{-2}]$ | $\Lambda^{-4} [\Lambda^{-2}]$ | Λ^{-2} | Λ^{-2} |
| C_{tu}^8, C_{td}^8 | Λ^{-2} | — | — | — | — | Λ^{-2} | — |
| $C_{Qq}^{1,1}$ | $\Lambda^{-4} [\Lambda^{-2}]$ | — | — | — | — | $\Lambda^{-4} [\Lambda^{-2}]$ | $\Lambda^{-4} [\Lambda^{-2}]$ |
| $C_{Qq}^{3,1}$ | $\Lambda^{-4} [\Lambda^{-2}]$ | Λ^{-2} | — | Λ^{-2} | Λ^{-2} | $\Lambda^{-4} [\Lambda^{-2}]$ | $\Lambda^{-4} [\Lambda^{-2}]$ |
| C_{tu}^1, C_{td}^1 | $\Lambda^{-4} [\Lambda^{-2}]$ | — | — | — | — | $\Lambda^{-4} [\Lambda^{-2}]$ | — |
| C_{Qu}^8, C_{Qd}^8 | Λ^{-2} | — | — | — | — | Λ^{-2} | — |
| C_{tq}^8 | Λ^{-2} | — | — | — | — | Λ^{-2} | Λ^{-2} |
| C_{Qu}^1, C_{Qd}^1 | $\Lambda^{-4} [\Lambda^{-2}]$ | — | — | — | — | $\Lambda^{-4} [\Lambda^{-2}]$ | — |
| C_{tq}^1 | $\Lambda^{-4} [\Lambda^{-2}]$ | — | — | — | — | $\Lambda^{-4} [\Lambda^{-2}]$ | $\Lambda^{-4} [\Lambda^{-2}]$ |
| $C_{\phi Q}^-$ | — | — | — | Λ^{-2} | — | Λ^{-2} | — |
| $C_{\phi Q}^3$ | — | Λ^{-2} | Λ^{-2} | Λ^{-2} | Λ^{-2} | — | — |
| $C_{\phi t}$ | — | — | — | Λ^{-2} | — | Λ^{-2} | — |
| $C_{\phi tb}$ | — | Λ^{-4} | Λ^{-4} | Λ^{-4} | Λ^{-4} | — | — |
| C_{tZ} | — | — | — | Λ^{-2} | — | Λ^{-2} | — |
| C_{tW} | — | Λ^{-2} | Λ^{-2} | Λ^{-2} | Λ^{-2} | — | — |
| C_{bW} | — | Λ^{-4} | Λ^{-4} | Λ^{-4} | Λ^{-4} | — | — |
| C_{tG} | Λ^{-2} | $[\Lambda^{-2}]$ | Λ^{-2} | — | $[\Lambda^{-2}]$ | Λ^{-2} | Λ^{-2} |

Table 1. Wilson coefficients in our analysis and their contributions to top-quark observables via SM-interference (Λ^{-2}) and via dimension-6 squared terms only (Λ^{-4}). A square bracket indicates that the Wilson coefficient contributes via SM-interference at NLO QCD. All quark masses except m_t are assumed to be zero. ‘Single t ’ stands for s - and t -channel electroweak top production.

Theoretical Framework

- We use an EFT description to parametrise deviations from the SM

| Relevant Operators | | | |
|--------------------|--|--------------------|---|
| Coefficient | Operator | Coefficient | Operator |
| $C_{\varphi Q}^1$ | $(\bar{Q}\gamma^\mu Q) (\varphi^\dagger i \overleftrightarrow{D}_\mu \varphi)$ | $C_{\varphi Q}^3$ | $(\bar{Q}\tau' \gamma^\mu Q) (\varphi^\dagger i \overleftrightarrow{D}'_\mu \varphi)$ |
| $C_{\varphi t}$ | $(\bar{t}\gamma^\mu t) (\varphi^\dagger i \overleftrightarrow{D}_\mu \varphi)$ | $C_{\varphi b}$ | $(\bar{b}\gamma^\mu b) (\varphi^\dagger i \overleftrightarrow{D}_\mu \varphi)$ |
| $C_{t\varphi}$ | $(\bar{Q}t) (\varepsilon \varphi^* \varphi^\dagger \varphi)$ | C_{tG} | $(\bar{t}\sigma^{\mu\nu} T^A t) (\varepsilon \varphi^* G_{\mu\nu}^A)$ |
| C_{tW} | $(\bar{Q}\tau' \sigma^{\mu\nu} t) (\varepsilon \varphi^* W_{\mu\nu}^I)$ | C_{tB} | $(\bar{Q}\sigma^{\mu\nu} t) (\varepsilon \varphi^* B_{\mu\nu})$ |
| $C_{qq}^{1(ijkl)}$ | $(\bar{q}_i \gamma^\mu q_j)(\bar{q}_k \gamma_\mu q_l)$ | $C_{qq}^{3(ijkl)}$ | $(\bar{q}_i \tau' \gamma^\mu q_j)(\bar{q}_k \tau' \gamma_\mu q_l)$ |
| $C_{uu}^{(ijkl)}$ | $(\bar{u}_i \gamma^\mu u_j)(\bar{u}_k \gamma_\mu u_l)$ | $C_{ud}^{8(ijkl)}$ | $(\bar{u}_i \gamma^\mu T^A u_j)(\bar{d}_k \gamma_\mu T^A d_l)$ |
| $C_{qu}^{8(ijkl)}$ | $(\bar{q}_i \gamma^\mu T^A q_j)(\bar{u}_k \gamma_\mu T^A u_l)$ | $C_{qd}^{8(ijkl)}$ | $(\bar{q}_i \gamma^\mu T^A q_j)(\bar{d}_k \gamma_\mu T^A d_l)$ |
| C_{lQ}^1 | $(\bar{Q}\gamma_\mu Q) (I\gamma^\mu I)$ | C_{lQ}^3 | $(\bar{Q}\tau' \gamma_\mu Q) (I\tau' \gamma^\mu I)$ |
| C_{lt} | $(\bar{t}\gamma_\mu t) (I\gamma^\mu I)$ | C_{lb} | $(\bar{b}\gamma_\mu b) (I\gamma^\mu I)$ |
| C_{eQ} | $(\bar{Q}\gamma_\mu Q) (\bar{e}\gamma^\mu e)$ | C_{et} | $(\bar{t}\gamma_\mu t) (\bar{e}\gamma^\mu e)$ |
| C_{eb} | $(\bar{b}\gamma_\mu b) (\bar{e}\gamma^\mu e)$ | - | - |

Theoretical Framework

- The Wilson coefficients are fitted are:

| Coefficients Fitted | | | |
|---------------------|---|---|---|
| 2-quark | C_{tG} $C_{\varphi t}$ – | $C_{\varphi Q}^3$ $C_{\varphi b}$ $C_{t\varphi}$ | $C_{\varphi Q}^- = C_{\varphi Q}^1 - C_{\varphi Q}^3$ $C_{tZ} = c_W C_{tW} - s_W C_{tB}$ C_{tW} |
| 4-quark | $C_{tu}^8 = \sum_{i=1,2} 2C_{uu}^{(i33i)}$ $C_{Qu}^8 = \sum_{i=1,2} C_{qu}^{8(33ii)}$ – | $C_{td}^8 = \sum_{i=1,2,3} C_{ud}^{8(33ii)}$ $C_{Qd}^8 = \sum_{i=1,2,3} C_{qd}^{8(33ii)}$ – | $C_{Qq}^{1,8} = \sum_{i=1,2} C_{qq}^{1(i33i)} + 3C_{qq}^{3(i33i)}$ $C_{Qq}^{3,8} = \sum_{i=1,2} C_{qq}^{1(i33i)} - C_{qq}^{3(i33i)}$ $C_{tq}^8 = \sum_{i=1,2} C_{uq}^{8(ii33)}$ |
| 2-quark 2-lepton | C_{eb} C_{lb} – | C_{et} C_{lt} – | $C_{IQ}^+ = C_{IQ}^1 + C_{IQ}^3$ $C_{IQ}^- = C_{IQ}^1 - C_{IQ}^3$ C_{eQ} |

$t\bar{t}H$ at lepton colliders

[1104.5132]

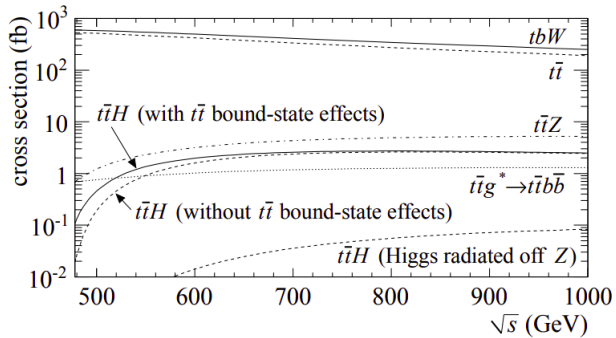


FIG. 2. Production cross section of the $e^+e^- \rightarrow t\bar{t}H$ signal (shown with and without $t\bar{t}$ bound-state effects), together with those of the main background processes, $t\bar{t}H$ (Higgs radiated off the Z boson), $t\bar{t}Z$, $t\bar{t}$, $t\bar{t}W^-/t\bar{t}W^+$ (denoted as $t\bar{t}W$), and $t\bar{t}g^* \rightarrow t\bar{t}bb$, as a function of the CM energy without beam polarizations. The initial state radiation and beamstrahlung effects are included.